

# Atmospheric Observations Made Using the *Aquameter* Water Band Radiometer<sup>1</sup>

A.J. LePage, A.T. Stair, Jr.  
Visidyne, Inc.  
10 Corporate Place  
South Bedford Street  
Burlington, MA 01803  
(781) 273-2820  
[lepage@visidyne.com](mailto:lepage@visidyne.com), [ats@visidyne.com](mailto:ats@visidyne.com)

A.P. Savin, V.F. Zakharenkov  
Kometa  
Velozazodskaya St. 5  
Moscow, Russia  
095 274-08-68  
[kometa@astroinform.ru](mailto:kometa@astroinform.ru)

**Abstract**—During late September and early October of 1998 the FISTA (*Flying Infrared Signatures Technology Aircraft*) aircraft made a series of three flights carrying a suite of instruments that included a Russian-built water band radiometer called the *Aquameter*. This instrument is designed to produce high spatial resolution imagery in four spectral bands in the M/LWIR (*Mid-Long InfraRed*). For these flights, three of the *Aquameter*'s spectral channels made observations in various parts of the water band from 5.4 to 7.2  $\mu\text{m}$  while the fourth channel observed to the ground in the 4.6 to 4.9  $\mu\text{m}$  band. The purpose of these flights was to obtain data to refine models of background clutter in support of instrument and experiment design for the RAMOS (*Russian American Observation Satellite*) program.

These radiometrically accurate multispectral images combined with data from other instruments, such as the PEELS (*Portable Eyesafe Environmental Lidar System*) lidar which supplied accurate data on cloud heights and composition, have allowed us to make important observations of the atmospheric structure as it appears in the M/LWIR and begin to identify the physical mechanisms responsible. Presented in this paper are a sample of our observations to date including imagery of various types of cloud structure and tropospheric waves observed in clear air with scales ranging from tenths to tens of kilometers visible in the water band.

## TABLE OF CONTENTS

1. INTRODUCTION
2. INSTRUMENTATION

3. OBSERVATIONS
4. CONCLUSIONS
5. ACKNOWLEDGEMENTS
6. REFERENCES
7. BIOGRAPHY

## 1. INTRODUCTION

Between September 21 and October 6, 1998 a series of six flights were made using the FISTA (*Flying Infrared Signatures Technology Aircraft*) to obtain data in support of future satellite experiment and instrument design efforts such as RAMOS (*Russian American Observation Satellite*). Three of these flights were categorized as "side-looking" flights designed to gather data on the polarization properties of solar radiation scattered from clouds in a number of infrared and visible wavelength bands simultaneously. These flights were a continuation of a program with the FISTA aircraft that began in 1997. The results of these earlier side-looking flights have been described elsewhere [1].

The other three flights had a new objective. They were "down-looking" flights where observations were made of a variety of natural backgrounds in and around the water absorption band in the M/LWIR (*Mid-Long InfraRed*). These measurements were expected to yield information on background clutter properties at these wavelengths and help verify predictions made by commonly used models such as MODTRAN.

<sup>1</sup> U.S. Government work not protected by U.S. copyright.

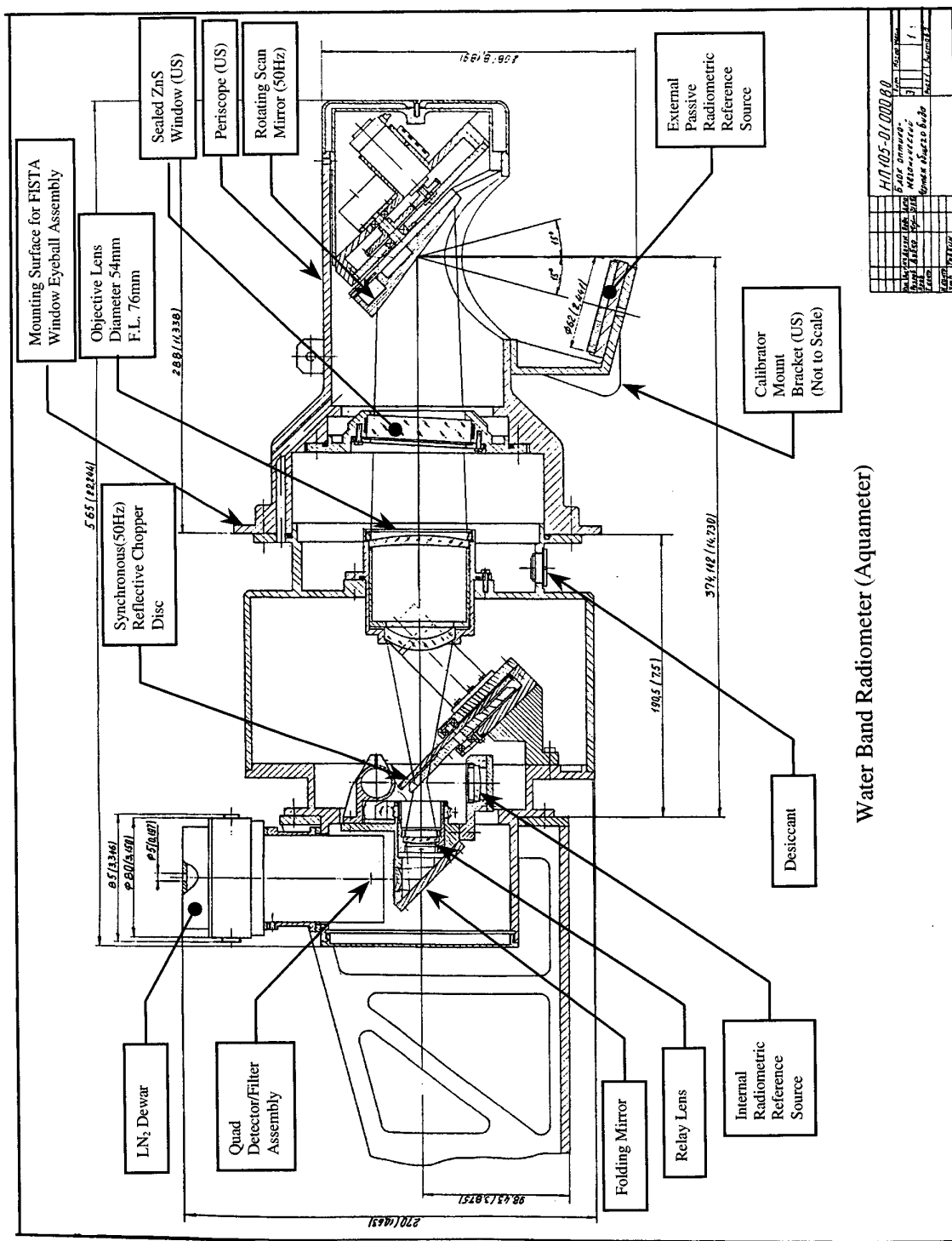
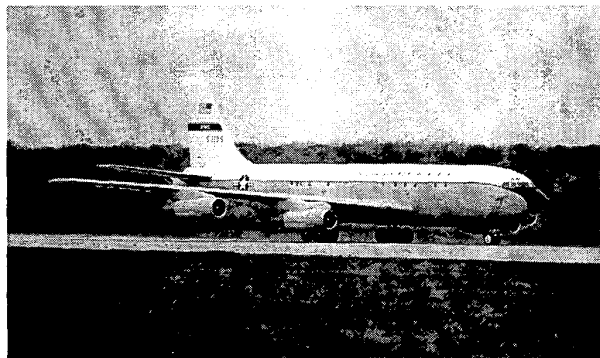


Figure 1 Diagram of Aquameter

The primary instrument for these down-looking flights was a water band imaging radiometer called the Aquameter shown in Figure 1. In this paper we will describe the Aquameter and the important supporting instruments that flew with it on FISTA during the 1998 campaign. We will then present samples of Aquameter image data and discuss the physical mechanisms responsible for what was observed.

## 2. INSTRUMENTATION

To obtain measurements for this program, we wanted to make use of existing assets to minimize development time and costs. The FISTA (*Flying Infrared Signatures Technology Aircraft*) aircraft, which we have used in past investigations, was an obvious choice [2]. The FISTA aircraft, shown in Figure 2, is a modified NKC-135E aerial refueling tanker (serial number 55-3135) built by Boeing that is based with the 452<sup>nd</sup> Test Squadron at Edwards AFB, California. It has a continuous flying time of 11 hours, a maximum range of about 11,000 km, and a maximum ceiling of 13,000 meters.



**Figure 2** FISTA aircraft

FISTA has been modified to act as a test bed for a wide variety of infrared and visible sensor systems. It has 20 windows on the starboard side of the fuselage with nearly all consisting of a 31.8 cm diameter clear aperture which are filled by a clear 1.9 cm thick Lexan window, an instrument window or periscope. The instruments, which can be run simultaneously, are mounted at these windows and look to the right during flight. Provisions also exist to mount periscopes in selected windows which allow the instrument to look in a variety of directions including fore, aft, up, and down.

The aircraft is also equipped with a GPS (Global Positioning System) to provide data on the position, heading and speed of the aircraft as well as its attitude. All this data along with a GPS-derived time base are recorded for later use in interpreting the data as well as geometrically correcting it for the motions of the FISTA aircraft and the shape of the Aquameter's unique scan pattern.

## Aquameter

Also known as the Water Band Radiometer (WBR), the Aquameter was the primary instrument of the three down-looking flights during the FISTA 98 campaign. Built by the Vavilov State Optical Institute in St. Petersburg, Russia, this instrument is a four-color quasi-conical scanner similar in design to those successfully used by Soviet Union and Russia for many decades [3]. The instrument, shown in Figure 1, has four HgCdTe detectors that use doping and optical filters integrated at the focal plane to simultaneously observe four different M/LWIR bands. The instrument is mounted in a standard FISTA 12-inch eyeball assembly with a modified 4 1/2-inch periscope. An inclined scanning mirror mounted in the periscope directs light from the scene being observed through a 76 mm focal length, f/1.4 lens which forms an image on the focal plane yielding a resolution of 4.4 mrad. The synchronized motion of the scanning mirror and other components allows the scene to be scanned at a rate of 50 Hz.

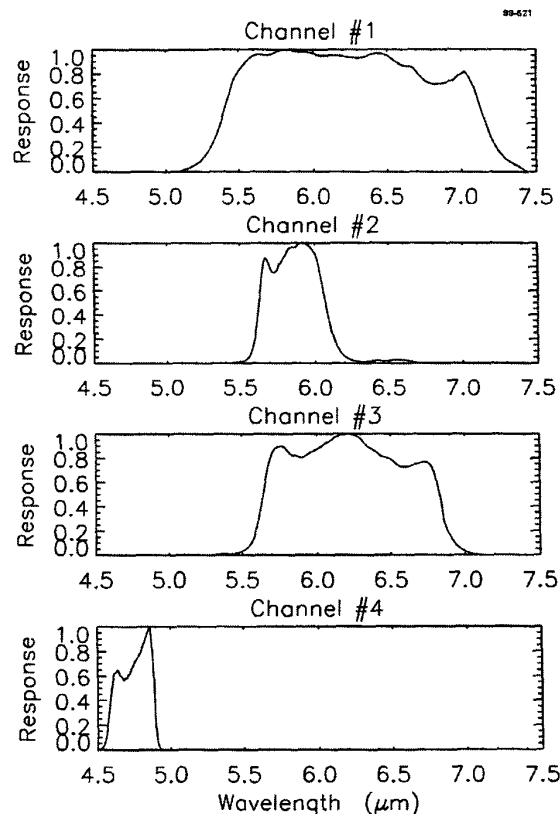


**Figure 3** Response functions of Aquameter spectral channels.

The spectral response functions for the Aquameter's four detectors are shown in Figure 3. Preflight estimates of the spectral band limits and noise equivalent radiances for each spectral channel are given in Table 1. Channel 1 covers the water absorption band in the M/LWIR and can view down to an altitude of about 5 km. The narrower spectral

responses of Channels 2 and 3, also in the water band, are designed to probe slightly different regions of the atmosphere and compliment the data from Channel 1. Channel 4 is not affected by atmosphere water vapor absorption and can view all the way through the atmosphere to the ground.

**Table 1** Aquameter Nominal Spectral Band Limits & NER

Channel Number	Nominal Band Limits (50% of Max)	Noise Equivalent Radiance (NER)
1	5.4 – 7.2 $\mu\text{m}$	0.20 $\mu\text{W}/\text{cm}^2\text{-sr}$
2	5.6 – 6.1 $\mu\text{m}$	0.30 $\mu\text{W}/\text{cm}^2\text{-sr}$
3	5.7 – 6.7 $\mu\text{m}$	0.15 $\mu\text{W}/\text{cm}^2\text{-sr}$
4	4.6 – 4.9 $\mu\text{m}$	0.02 $\mu\text{W}/\text{cm}^2\text{-sr}$

One of the unique attributes of the Aquameter is its scan pattern. Because of the tilt of the motorized scanning mirror, the scan pattern is roughly egg shaped with the long and short axes having a full width of about  $30^\circ$  and  $20^\circ$  respectively. The long axis is aligned perpendicular to the direction of travel and passes through the nadir point. The short axis is aligned parallel with the direction of travel and also passes through the nadir point. The point of the "egg" is oriented away from the aircraft. The shape of the full scan pattern is shown schematically in Figure 4.

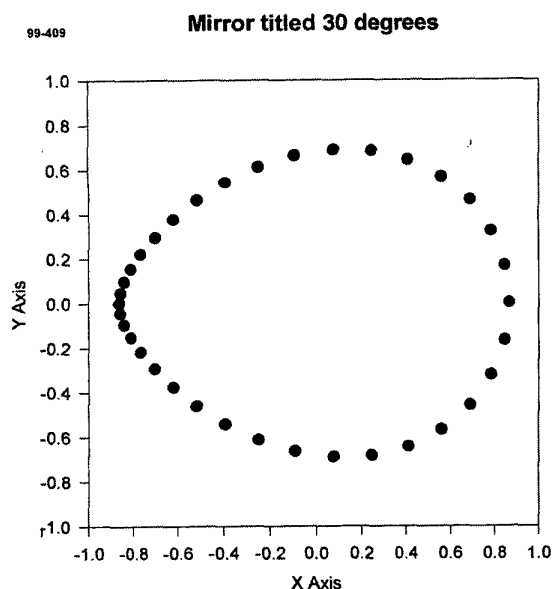


**Figure 4** Diagram of idealized Aquameter scan shape. The direction of travel is downwards.

Since all four detectors are offset from the optical axis of the system, the paths scanned by each detector across the scene are not identical. Combined with the forward motion of the aircraft as well as changes in its attitude normally encountered even during level flight, each detector describes a unique and complex pattern across the ground.

Because of the combination of the scan rate and forward motion of the aircraft, scans are spaced about 4 meters apart in the direction of flight (assuming a aircraft speed of about 200 m/s). This combined with the Aquameter's nominal 50-meter ground resolution at a height of 12 kilometers results in the instrument oversampling the scene at ground level by about a factor of 13 in the direction of flight or in-scan direction. Objects above the ground and closer to the aircraft can be imaged at resolutions better than the nominal 50-meter ground resolution. The four-meter spacing between scans approximately equals the instrument's resolution for objects about 1 km below the aircraft. Regardless of altitude, the Aquameter modestly oversamples in the cross-scan direction by a factor of about 1.7. This oversampling allows scenes to be recorded at the instrument's resolution limits for a wide range of altitudes and permits some measure of noise reduction through averaging during data analysis.

Another useful design feature of the Aquameter is its ability to obtain virtually simultaneous forward-looking and back-looking views of a scene. During normal operation, the Aquameter first records data for about a quarter of a full scan in the forward direction at an angle of up to about  $+11^\circ$  from nadir. After another quarter of a scan has passed with no data being recorded, the back scan at an angle of up to about  $-11^\circ$  from nadir is recorded. The shape of the forward and backward scan arcs as actually measured during post-flight calibration at the Space Dynamics Laboratory in Logan, UT are shown in Figure 5. During the last quarter of the scan, an external black body reference source is observed with 10 measurements being averaged and recorded along with the reference source's temperature. This information is later used in the calibration process.

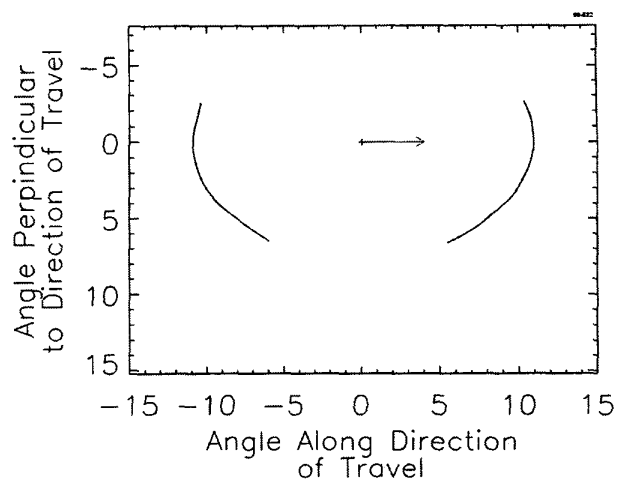


**Figure 5** Arcs over scan pattern where Aquameter gathers imaging data. The left arc is the back-looking scan and the right one is the forward-looking scan. The direction of travel is indicated by the arrow coming from the nadir point.

The ability to record a scene in this fashion allows triangulation of objects visible in the forward- and back-

scan images to be performed thus yielding their altitudes. For the analysis performed here, the following empirical relation was derived to roughly estimate the altitude of features seen near the center of the forward- and back-looking Aquameter image strips:

$$z = h - Cv\Delta t \quad (1)$$

where  $z$  is the altitude of the object (in meters),  $h$  is the altitude of the aircraft (in meters),  $v$  is the mean velocity of the aircraft (in meters/second), and  $\Delta t$  is the time delay of the visibility of the object as seen in the forward- and back-looking image strips (in seconds). The constant  $C = 3.05$  is derived empirically by comparing time delays with their actual altitudes derived from PEELS data. This method of estimating feature altitudes is used when PEELS is unavailable.

In principle it should also be possible to use these data to perform full stereo analysis of the scene provided that the appropriate photogrammetric information about the instrument and its scan pattern is available in addition to detailed information on the aircraft's position and attitude. Detailed stereo analysis is currently being studied by our colleagues at Astrophysica in Moscow. Simpler geometric transformation techniques have already been developed by Russian and American team members to take into account the gross effects of the Aquameter scan pattern shape and the motions of the aircraft. These techniques have proved sufficient for simple two-dimensional scene reconstruction and image analysis.

Normally eight 150-pixel wide image strips are produced by the Aquameter: One forward- and one back-looking view for each of the four spectral channels. These imaging data are recorded as a pair of electronic files with forward-looking data in one and back-looking data in the other. The latter file also contains information on the blackbody reference temperature required for the calibration procedure. Of the 150 pixels in the recorded image, typically a 142-pixel wide strip is actually usable and not corrupted by views of part of the instrument interior or aircraft. As much as six minutes of data (yielding four 150 by 18,000 pixel images) are recorded in each file.

Four different types of Aquameter data products were produced to support data analysis and the selection of scenes for further processing. To aid in a general overview of the large Aquameter data set, an atlas consisting of all the uncalibrated image strips was prepared for review by team members. A subset of these data were calibrated and included in a subsequent atlas along with PEELS lidar data to aid in further selection of scenes.

The third level of processing included suppression of various types of electronic noise in the data. Careful filtering in the Fourier and spatial domains along with the previously mentioned oversampling of the scene by the instrument (which allows averaging to further reduce

random noise) have allowed us to produce high fidelity scenes largely unaffected by noise. The various sources of noise have been identified based on a detailed analysis of the noise in the data and steps are being taken to eliminate it during future flights. These filtered scenes are of sufficient quality to perform various types of simple analysis without further processing. The final type of data product are those that have been calibrated, filtered, and geometrically transformed to take into account the shape of the Aquameter scan pattern and the motions of the aircraft. These final data products approximate the view of a frame camera at an assumed altitude and are accurate enough to perform most types of two-dimensional analysis.

#### *Michelson Interferometers*

For the FISTA 98 flights, the aircraft was equipped with a trio of Michelson interferometers supplied by the Air Force Research Laboratory (AFRL). These interferometers were designed to provide spectra with complementary properties in overlapping spectral regions ranging from the SWIR (Short Wave InfraRed) to M/LWIR. In order to provide supporting data for this program's polarization measurements, these instruments were modified with filters to provide information on the degree and angle of polarization as a function of wavelength for the side-looking missions. These same instruments operated in a non-polarization mode to provide spectra during the down-looking flights described here. Their data provided a check on the Aquameter's calibration that independently confirmed the 10% absolute radiometric accuracy of the instrument and data reduction procedures.

Interferometer 102 makes use of an InAs detector to produce spectra in the 1.5 to 3.1  $\mu\text{m}$  range with a resolution of 4  $\text{cm}^{-1}$ . It produces one spectrum each 1.1 second and has a circular field of view that is approximately 26 milliradians in diameter.

Interferometer 103 uses a HgCdTe detector to produce spectra in the 2 to 7  $\mu\text{m}$  range with a resolution of about 1  $\text{cm}^{-1}$ . Data supplied by Interferometer 103 was most valuable in verifying the calibration of the Aquameter. This instrument produces one spectrum each second and has a diamond-shaped field of view with each side being about 9 milliradians across.

Interferometer 105 uses an InSb detector to make spectral measurements in the 2.0 to 5.5  $\mu\text{m}$  range with a resolution of 1  $\text{cm}^{-1}$ . Like Interferometer 103, it makes one spectrum each second and has a field of view is about 17 milliradians in diameter. Unlike the other interferometers, 105 has not been used to make polarization measurements.

Raw spectral data from these instruments are recorded digitally along with measurement of calibration sources for post-flight processing. All three Michelson interferometers are equipped with their own dedicated video camera coaligned with each interferometer's field of view to

provide a record of what was observed at any given time. The fields of view of these instruments were roughly coincident with the Aquameter allowing direct comparison of measurements.

### PEELS

The next instrument that yielded valuable data for the FISTA 98 flights was PEELS (*Portable Eyesafe Environmental Lidar System*) built by Visidyne, Inc. PEELS made lidar soundings of the environment being observed, thus complimenting the observations of the other instruments.

Originally PEELS was designed as a portable, tripod-mounted lidar system meant to obtain range and depolarization measurements of various types of clouds and aerosols within its nominal 25 kilometer range [4]. Because of its design and the wavelength employed, it has been rated as eyesafe and skinsafe. For the FISTA flights PEELS was modified to operate using a single optical aperture (as opposed to the separate transmitting and receiving optics it normally uses) and repackaged to conform to the aircraft's instrument interface standards.

The transmitter for PEELS is a Nd:YAG pulsed laser with a KTP OPO operating at a wavelength of 1.574  $\mu\text{m}$ . For the FISTA flights, the output beam was vertically polarized. The typical laser pulse has an energy of 45 millijoules and a width of 10 nanoseconds. The maximum repetition rate for the laser is 10 Hz and the nominal beam divergence is 0.5 milliradians. The receiver on PEELS is a commercially available 20-cm Schmidt-Cassegrain telescope with a pair of InGaAs detectors fitted with polarizing filters. Its field of view, which roughly matches the region of laser illumination, is about 1 milliradian.

The range resolution of the system is variable and can be as small as 8 meters. For the FISTA 98 observations, resolution was set at 150 meters and as many as 100 soundings were averaged to yield each measurement. Typically only 30 shots (or 3 seconds of data) were averaged yielding an effective footprint that was ~600 meters long in the direction of travel.

PEELS performs measurements of range and backscatter depolarization only. The range measurement is based on the round trip time of the laser pulse. The percent depolarization is measured by taking the ratio between the horizontal polarization component of the return signal and the sum of the vertical and horizontal polarization return signals. This quantity provides an independent method for determining the composition of the clouds being observed [5].

For the down-looking flights described here, PEELS was mounted so that it was viewing  $+13^\circ$  from nadir (i.e. in the direction of travel). This roughly corresponded to the  $+11^\circ$  maximum viewing angle of the Aquameter forward scan

allowing PEELS to provide direct measurements of cloud range and composition. The PEELS range measurements were remapped using aircraft position and attitude data as a function of time and altitude above sea level that could be directly compared with the Aquameter's forward scan images.

### 3. OBSERVATIONS

The three down-looking FISTA 98 flights were Flight 9826 flown on September 28, 1998, Flight 9827 on September 30, and Flight 9901 on October 2. As discussed earlier, the primary instrument for the down-looking flights was the Aquameter. The PEELS lidar provided range and depolarization measurements of the clouds observed. Other instruments operating at visible and IR wavelengths provided ancillary data on the scenes being observed.

Ideally we wanted to have simultaneous PEELS and Aquameter data to aid in the interpretation of what was being seen. The ultimate goal was to select a limited set of "scenes" that displayed a range of background structure and boundaries (e.g. the boundary between the ground and clouds or between clouds of various altitudes or compositions). A variety of problems prevented us from securing PEELS lidar data for Flight 9826 and limited us to obtaining only about an hour's worth of data each from Flights 9827 and 9901.

While these problems were solved in time for the side-looking flights that followed, the limited availability of PEELS data in a way helped to narrow the focus of our initial Aquameter data analysis effort. Fortunately there were a wide variety of conditions observed during the time periods where both PEELS and Aquameter were available during Flights 9827 and 9901. As a result, the limits on the amount of PEELS data available for the down-looking flights had no impact on meeting this experiment's goals.

While we will confine ourselves to discussing initial analysis of this limited data set in this paper, use of simple triangulation between objects seen in the forward- and back-looking scans of the Aquameter images yields reasonably accurate estimates of cloud heights when PEELS lidar data is not available. This will allow us to eventually use all the Aquameter data from Flight 9826 and the balance of the data from Flights 9827 and 9901 in future analysis.

Flight 9827 took place off the Pacific coast of California. During this flight, PEELS obtained a total of 1,033 soundings representing 51 minutes 39 seconds of data obtained between 00:15:48 UT and 01:27:44 UT on October 1, 1998 resulting in 72% coverage during this time period. The first half of PEELS data from this flight mapped as a function of time and altitude above sea level is shown in Figure 6. Vertical white bars in this and subsequent illustrations of PEELS data represent data gaps. This segment of data is dominated by a low marine cloud layer at an altitude of about 1 km.

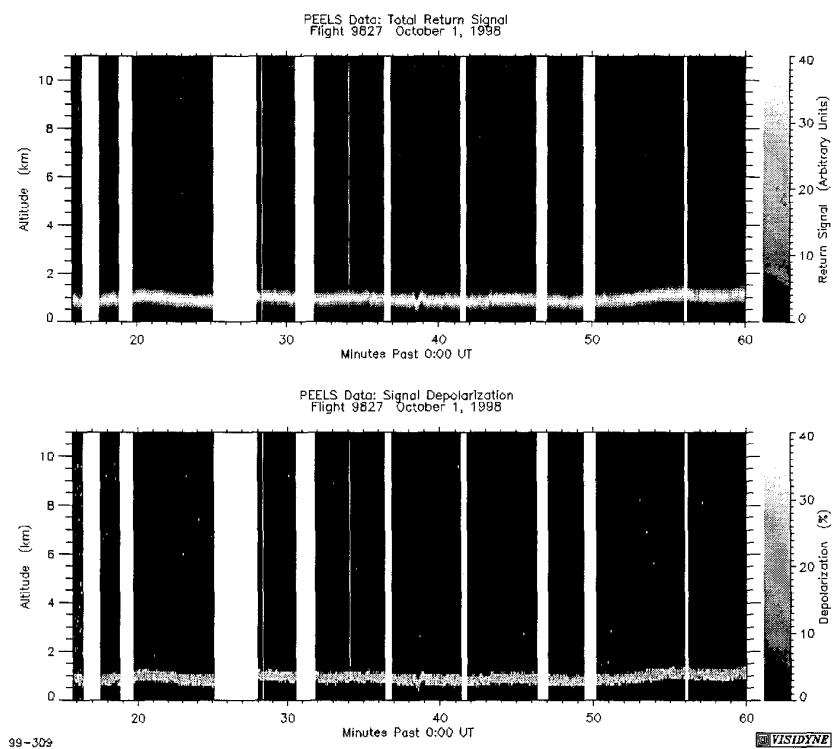


**Figure 6** First half of PEELS lidar data for Flight 9827

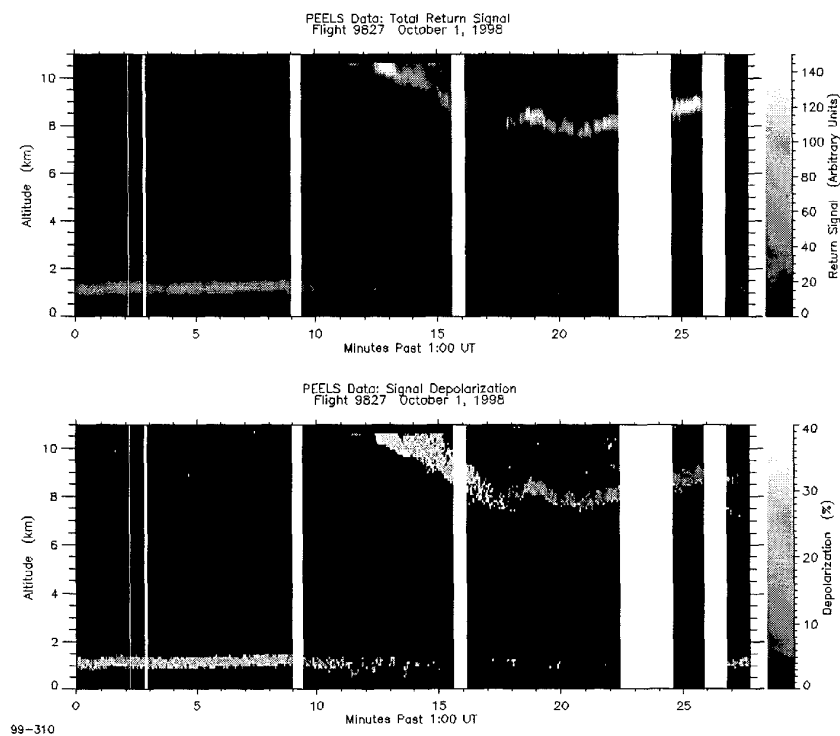


**Figure 7** Second half of PEELS lidar data for Flight 9827

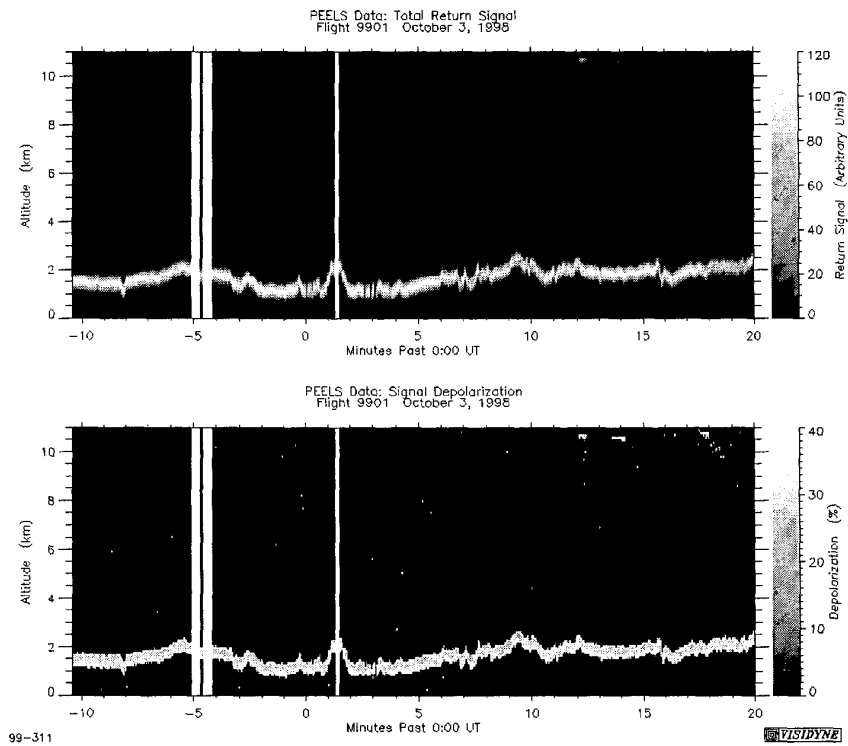


**Figure 8** First half of PEELS lidar data for Flight 9901

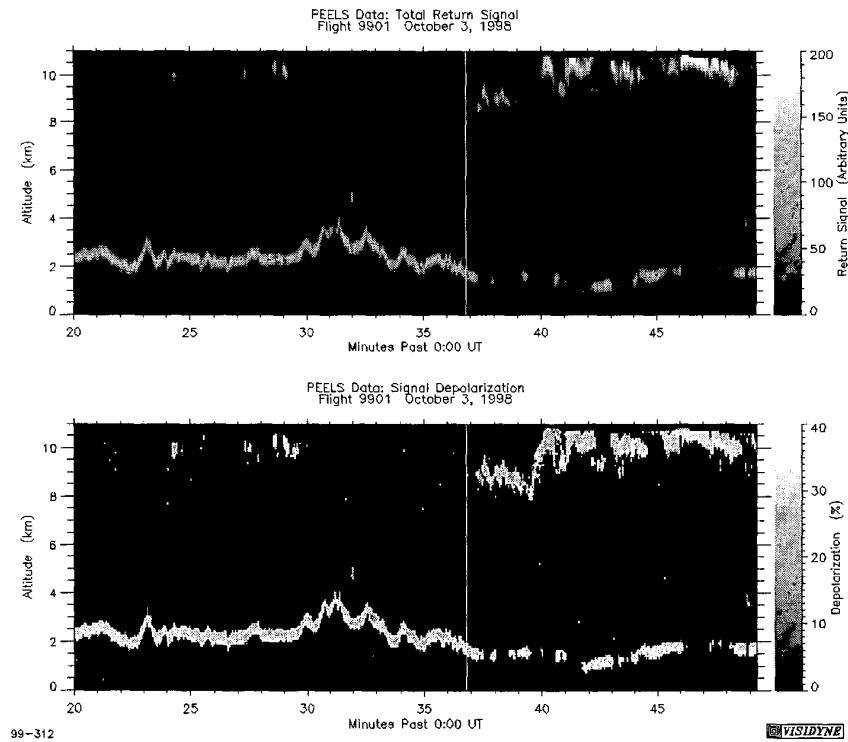


**Figure 9** Second half of PEELS lidar data for Flight 9901



A much more interesting segment of PEELS data is shown in Figure 7. Again the marine cloud layer at 1 kilometer dominates at low altitude but at about 1:12 UT, FISTA passed through a high altitude cirrus cloud layer which itself was decreasing in altitude at a rate of 1 km for every 19 km traveled by FISTA. The marine cloud layer is still visible on occasions through thin spots in this cirrus cloud layer.

At about 1:18 UT this cirrus cloud layer undergoes an abrupt change. It becomes optically thicker and the sharp decrease in the PEELS signal depolarization indicates a change in composition from ice to water. This transition is also marked by a slight increase in cloud altitude from about 7.8 to 8.5 km. This water cloud layer slowly increases in altitude reaching 9 km before thinning out at about 1:27 UT after which we reach the end of the PEELS data set for this flight.

Flight 9901 took place over the American southwest. Starting at Edwards AFB, CA, the flight proceeded to Pueblo, CO then on to Cheyenne, WY. This was followed by a return to Colorado and a pass over Denver on the way to Wichita Falls, TX with a subsequent return to Edwards AFB.

During this flight, PEELS obtained a total of 999 soundings representing 49 minutes 57 seconds of data obtained between 23:49:36 UT on October 2, 1998 and 00:49:19 UT on October 3, 1998 resulting in 84% coverage during this time period. The first half of PEELS data from this flight is shown in Figure 8. This segment of data is dominated by views of the ground showing the rough topography of the American southwest with no clouds initially visible. Checks of the elevation of selected topographic features found by PEELS with those on USGS maps indicates that PEELS is providing accurate altitude measurements. Starting around 00:12 UT, some thin, high altitude cirrus clouds and/or contrails are occasionally observed.

The second segment of PEELS data from Flight 9901, shown in Figure 9, continues to show the ground but also more high altitude clouds. At first there are some high ice clouds and contrails like before but by 00:37 UT a more expansive deck of clouds displaying a range of altitudes and opacities is observed. The ground continues to be visible through thin spots and breaks in this cloud deck which is seen to the end of this PEELS data set.

Based on a review of PEELS and Aquameter data, a limited number of one- to two-minute scenes from Channel #1 and #4 forward scans were initially selected for calibration and filtering. These were subsequently analyzed in detail. A subset of these were geometrically transformed to correct for the shape of the Aquameter's scan pattern in order to aid more detailed spatial analysis.

#### *Cloud Edges*

One of the primary goals of these experiments was to determine the characteristics of cloud edges and how their appearance changes as a function of wavelength used to make the observations. During the examination of the Aquameter data sets, two basic types of cloud edges were noted: Clouds with edges that appeared sharp regardless of wavelength used to observe them and clouds with diffuse edges whose appearance depended strongly on the wavelength used to observe them.

An example of a cloud deck with sharp edges is shown in Figures 10 and 11. Figure 10 gives a synoptic view of the area. The top and middle panels show calibrated Aquameter forward-looking image strips for Channels 1 and 4 respectively. These images have not been filtered or geometrically transformed to correct for the Aquameter scan pattern or movements of the aircraft. They are shown simply as a function of time and image row number. The bottom panel shows the PEELS lidar data for the time period covered by the Aquameter images.

These image strips are from Flight 9827 and cover the time period from about 1:15:45 to 1:21:45 UT on October 1, 1998 when the FISTA aircraft was over the Pacific Ocean off the California coast. It shows the section of data where the high clouds at an altitude of 8.5 km which partially obscures the view of the low marine cloud layer change from a thin ice cloud to a optically denser water cloud. As expected, Channel 1, which can not see below about 5 km, does not see the low marine cloud layer while it is visible in Channel 4. The higher altitude clouds are clearly visible in both channels.

Also visible in the scene, especially in the Channel 1 image, are a series of dark vertical bands. Triangulation performed on the images of these bands from the Aquameter's forward- and back-scans using Equation 1 indicates that these are clouds or contrails some 375 meters below the aircraft at an altitude of about 12.1 kilometers. This is too close to be observed by PEELS as configured for the FISTA 98 missions.

Figure 11 shows a close-up view of the cloud edge that has been filtered and geometrically transformed to correct for the Aquameter's scan pattern shape. The image, which represents about 39 seconds of data centered on about 1:18:45 UT, was produced assuming that the cloud deck and aircraft altitudes are 8.5 and 12.4 kilometers, respectively and has been remapped on a 10-meter grid (the approximate resolution limit of the Aquameter at that range). The top and middle panels are images from Channel 1 and 4, respectively, while the bottom panel shows the ratio of the Channel 1 image to the Channel 4 image. Faint arcs seen in the first two kilometers of the Channel 1 image are nearby contrails or clouds that have been distorted by the transformation process.

PEELS & Calibrated Aquameter Data  
Flight 9827 October 1, 1998  
plt23f.011

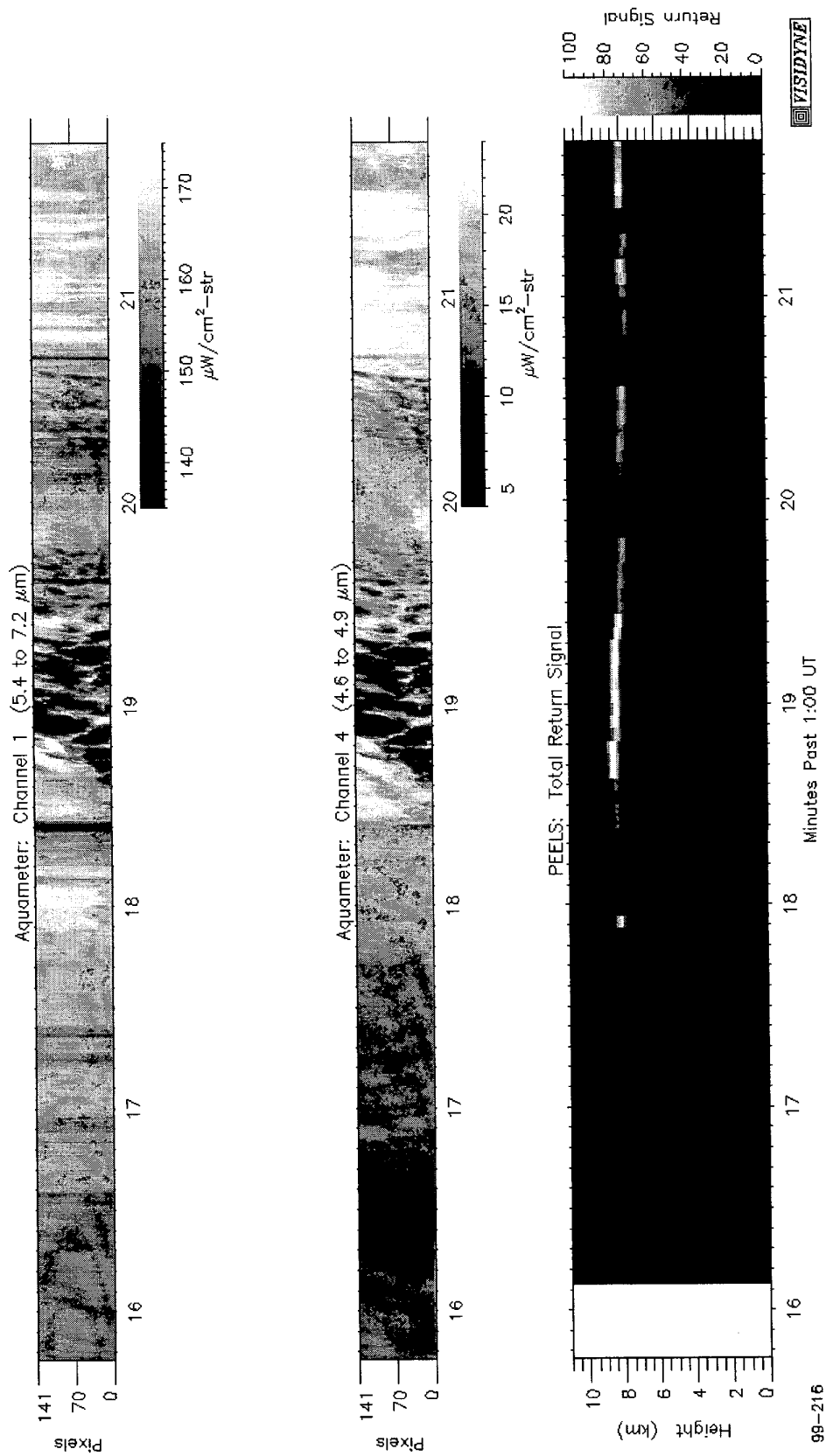
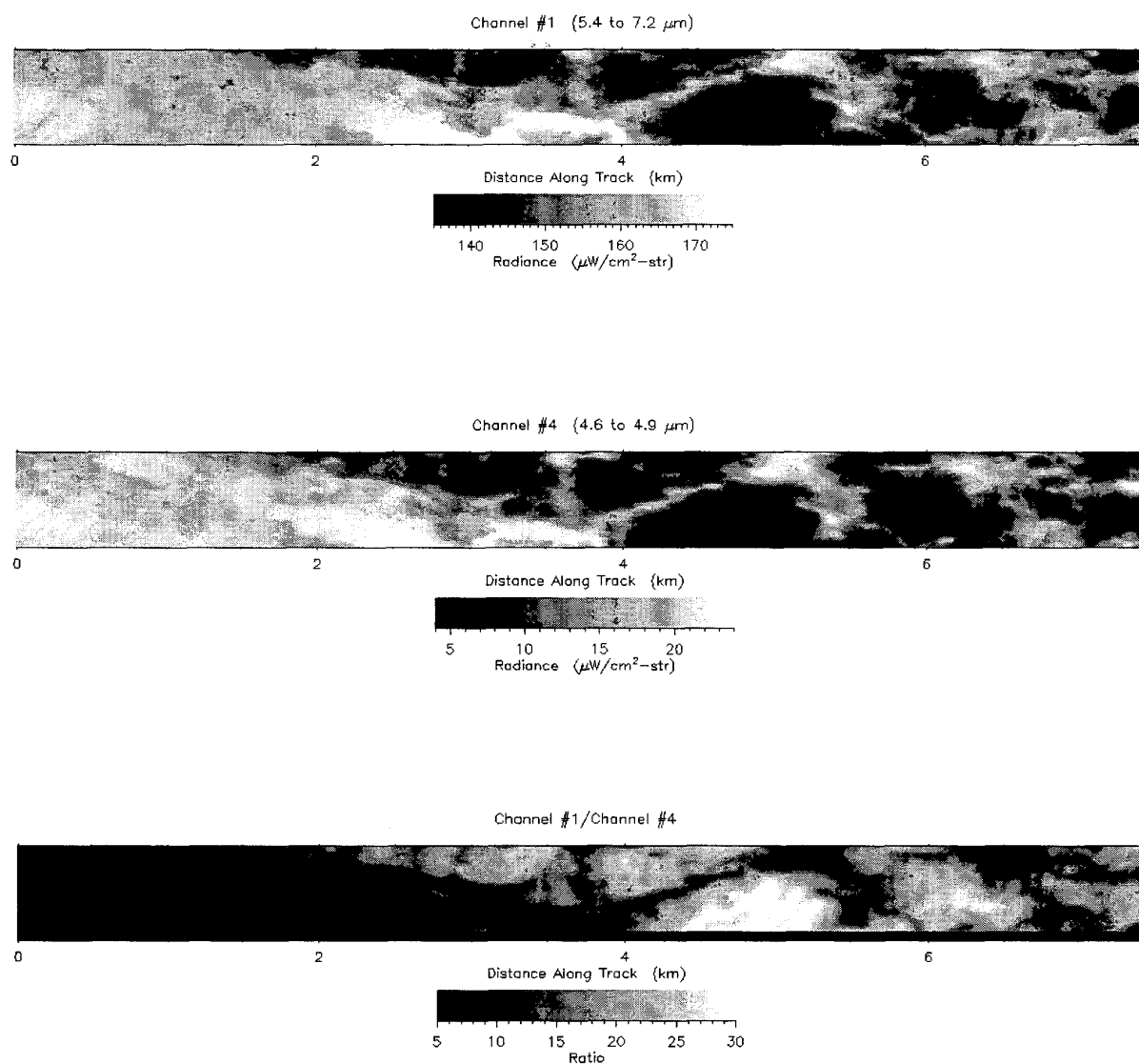


**Figure 10** Example of cloud with "sharp" edges. The top two image strips are calibrated, unfiltered forward-looking Aquameter images from Channels 1 (top panel) and Channel 4 (middle panel) that have not been geometrically transformed. They are shown as a function of time and image row number. The dark vertical bands especially visible in the Channel 1 image are isolated clouds distorted by their proximity to the aircraft. The bottom panel shows the corresponding PEELS lidar data as a function of time and altitude above sea level.

Scene #2 Flight 9827 October 1, 1998 ~01:18:30 UT  
 Filtered Calibrated First Order Scan Pattern Correction  
 10 m Grid Assumed 8.5 km Feature Altitude



98-484

VISIDYNE

**Figure 11** Calibrated, filtered, and geometrically transformed Aquameter images showing details of sharp cloud edges. The images were reconstructed with the assumption that the cloud deck and aircraft are at altitudes of 8.5 and 12.4 kilometers respectively. The top panel shows Channel 1 and the middle panel shows Channel 4. The bottom panel is the simple ratio of the radiance values (on a pixel by pixel basis) of Channel 1 to Channel 4.

PEELS & Calibrated Aquameter Data  
Flight 9901 October 3, 1998  
plt31f.012

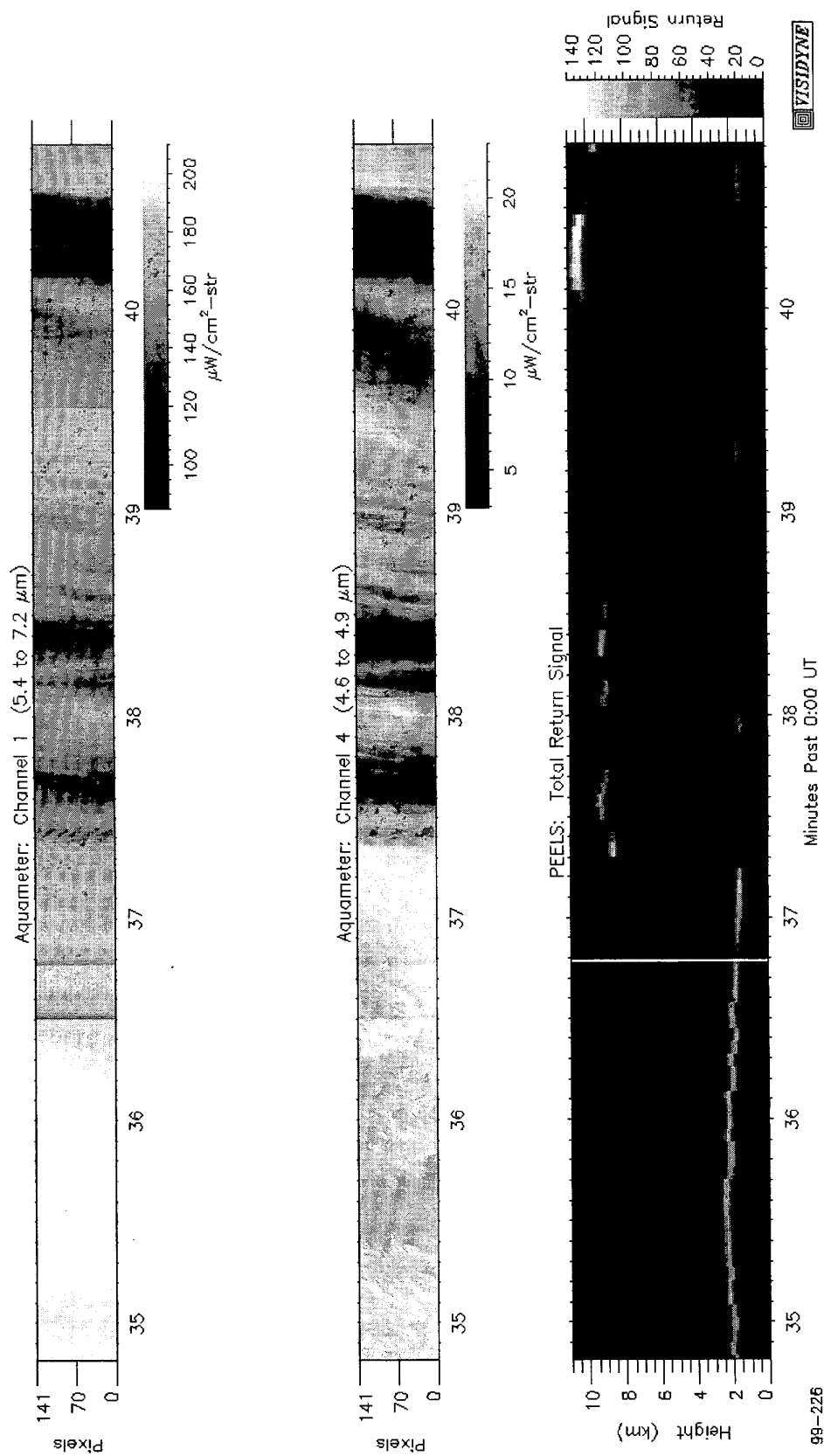
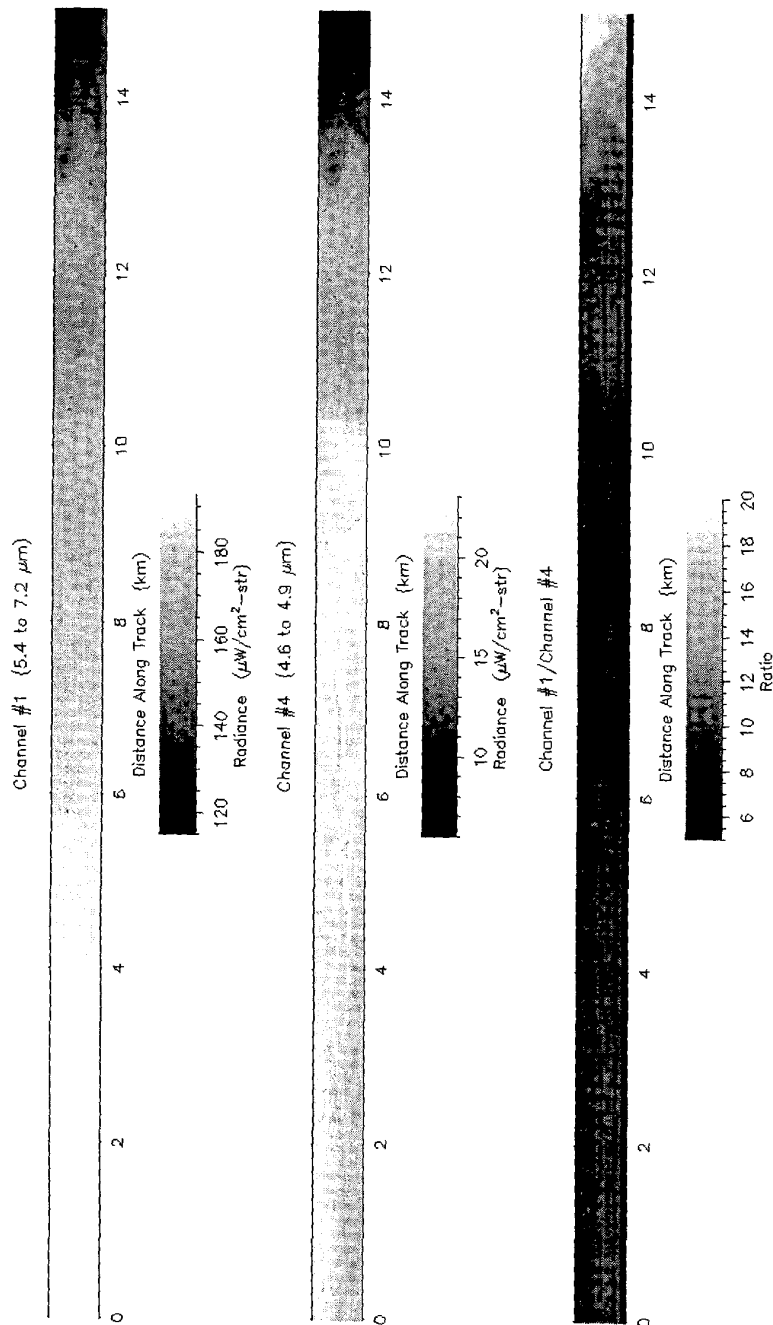


**Figure 12** Example of cloud with "diffuse" edges. The top two image strips are calibrated, unfiltered forward-looking Aquameter images from Channels 1 (top panel) and Channel 4 (middle panel) that have not been geometrically transformed. They are shown as a function of time and image row number. The pair of vertical bands between 00:36:30 and 00:37:00 UT are the result of noise in the reference body temperature used to radiometrically calibrate the images. The bottom panel shows the corresponding PEELS lidar data as a function of time and altitude above sea level.

Scene #3 Flight 9901 October 3, 1998 00:37:00 UT  
 Filtered, Calibrated First Order Scan Pattern Correction  
 25 m Grid Assumed 8.5 km Feature Altitude



99-485

VISIDINE

**Figure 13** Calibrated, filtered, and geometrically transformed Aquameter images showing diffuse cloud edges. The images were reconstructed with the assumption that the cloud deck and aircraft are at altitudes of 8.5 and 12.2 kilometers respectively. The top panel shows Channel 1 and the middle panel shows Channel 4. The bottom panel is the simple ratio of the radiances (on a pixel by pixel basis) in Channel 1 to Channel 4.

As can be seen, the leading edge of these clouds is very sharp and appear almost identical in the two spectral channels. The high ratio values (up to about 30) in the denser parts of the cloud are consistent with that expected from an optically dense, cold cloud.

Figures 12 and 13 illustrate a scene with clouds with more diffuse edges. Figure 12 gives a synoptic view of the scene with calibrated, unfiltered Channel 1 and 4 forward-looking image strips and PEELS lidar data similar to Figure 10.

These image strips are from Flight 9901 and cover the time period from about 00:34:50 to 00:40:50 UT on October 3, 1998 when the FISTA aircraft was over the southeastern Utah. It shows the section of data where the transition is made from viewing the ground to a fairly dense cloud deck composed of ice at an altitude of about 8.5 km. The ground can be seen in Channel 4 with details being clearly visible.

While the ground can not be seen in Channel 1 (as expected), the start of the high altitude cloud deck is visible in both spectral channels starting at about 00:37:20 UT. Vertical lines especially visible in Channel 1 at 00:36:30 UT, 00:36:47 UT, and 00:39:31 UT in Figure 12 are artifacts from reference temperature transients that were corrected during subsequent filtering.

Figure 13 shows a close-up view of this cloud edge that has been filtered and geometrically transformed to correct for the Aquameter's scan pattern shape. The image, which represents about 59 seconds of data centered on about 00:37:00 UT, was produced assuming that the cloud deck and aircraft altitudes are 8.5 and 12.2 kilometers, respectively and has been remapped on a 25-meter grid.

In the Channel 4 image, which is not affected by atmospheric water vapor, the cloud edge is clearly visible about 10 kilometers into the image. In the Channel 1 image which is affected by atmospheric water vapor, the radiance slowly starts to fall off (and the ratio with Channel 4 decreases) starting at about 4 kilometers into the image strip and decreases significantly at the edge of the cloud as visible in Channel 4. The corresponding portion of the Channel 4 image shows no decrease in radiance in the 6 kilometer stretch preceding the apparent edge of the cloud. This distinct difference in the appearance of the cloud edge as a function of wavelength is of interest. Further into the cloud, the density of the cloud increases and the ratio of Channel 1 to Channel 4 radiances reaches as high as 20 which is expected from an optically dense, cold cloud.

Examination of visible imagery shows evidence of a faint haze that is barely visible in the PEELS lidar data. It is possible that there are enhanced levels of water vapor associated with this thin haze. If the haze particles are very small, they would scatter visible light ( $\lambda \approx 0.5 \mu\text{m}$ ) effectively but allow longer MWIR wavelengths like those observed by Channel 4 ( $\lambda \approx 4.8 \mu\text{m}$ ) to pass through unimpeded.

There could be water vapor associated with this thin haze layer which would cause the observed decrease in radiance in the water vapor band as observed in Channel 1. With these interesting examples in hand, our examination of cloud edges as seen in the Aquameter data set will continue.

### *Tropospheric Waves*

Among the more surprising results from the FISTA 98 campaign were observations in clear air of tropospheric waves in the 7 to 9 kilometer altitude range that were visible only in the water band images. These waves do not appear in images from Channel 4 which can see to the ground nor does the PEELS lidar data indicate the presence of clouds that could cause the observed variations in background radiance. While we are still studying the phenomenon and attempting to determine its cause, we believe that they may be manifestations of gravity waves.

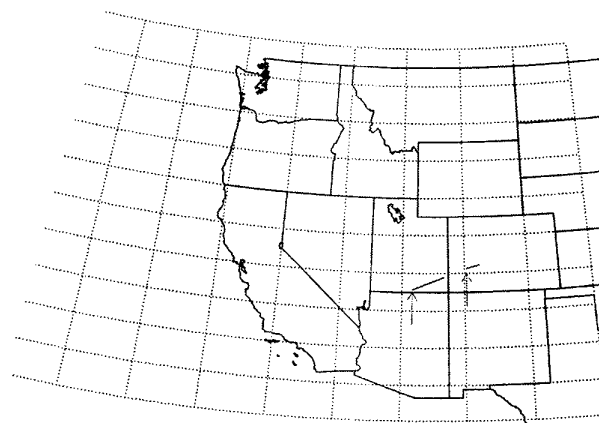


**Figure 14** Location of waves observed with 10-kilometer scales during flight 9901.

The largest size waves observed during the FISTA 98 flights were seen during Flight 9901 from about 23:57 to 00:13 UT and 00:22 to 00:27 UT on October 2-3, 1998. These times correspond to when the FISTA aircraft was flying over southeastern Utah and southwestern Colorado as shown in Figure 14.

An example of these waves is shown in Figure 15. This is a calibrated, unfiltered forward-looking image from Channel 1. Small scale vertical structures in the image are instrument noise which have not been removed. This 62-kilometer long image strip is from data taken between about 23:57:30 UT on October 2, 1998 and 00:03:00 UT October 3 – about 5 ½ minutes of data.

Clearly evident in this image are semi-periodic variations in background radiance with trough-to-peak amplitudes as large as ~12%. The spacing of the wave crests ranges from 7 to 14 kilometers in the direction of travel with a mean on the order of 10 kilometers. Waves of similar size with a comparable amplitude in radiance variation were observed throughout the previously stated time period.

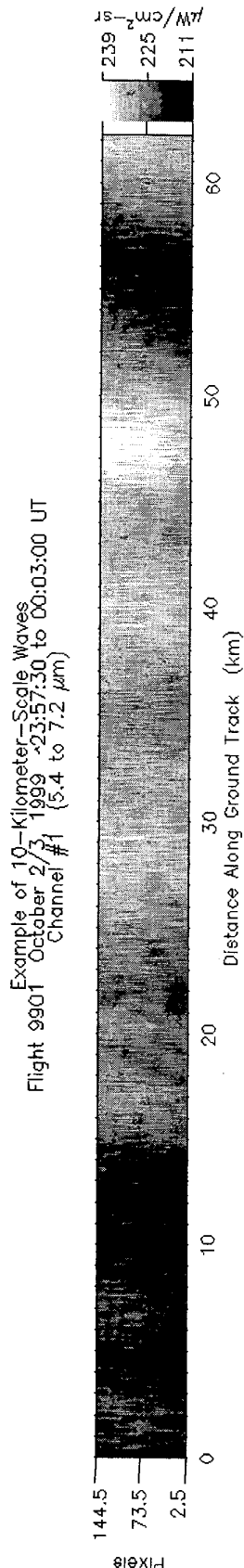


**Figure 15** Calibrated, unfiltered Channel 1 forward-looking Aquameter image of 10-kilometer-scale waves observed during Flight 9901 in southeastern Utah near 00:00 UT on October 3, 1998. Faint, small-scale vertical structures in the image is instrument noise.

Scene #7 Flight 9827 October 1, 1998 00:32:30 UT  
 Filtered Calibrated First Order Scan Pattern Correction  
 25 m Grid Assumed 7.2 km Feature Altitude

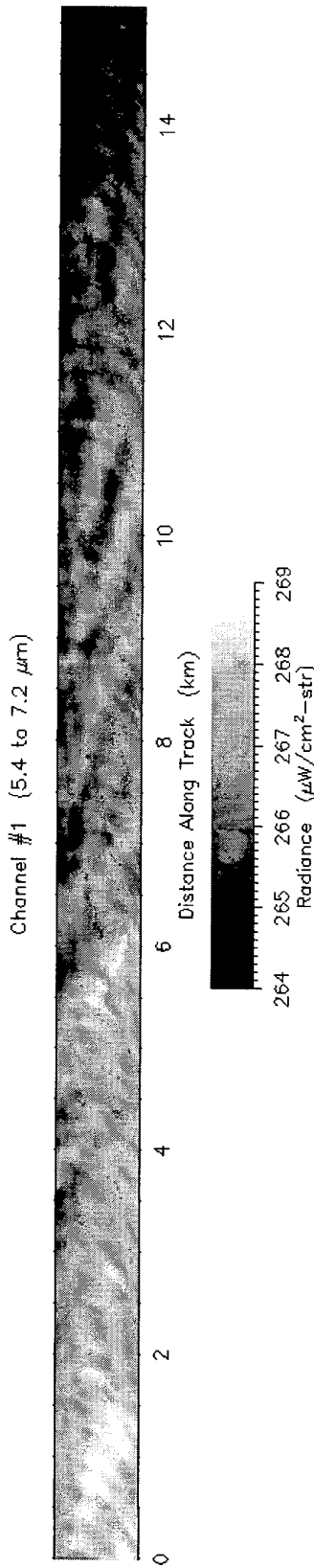


**Figure 16** Calibrated, filtered and geometrically transformed Channel 1 forward-looking Aquameter image of subkilometer-scale waves observed during Flight 9826 over the Pacific Ocean off the coast of California near 00:32:30 UT on October 1, 1998. The assumed wave and aircraft altitudes are 7.2 and 12.1 kilometers respectively. Faint arcs are residual noise artifacts distorted by the geometric transformation process that have been made visible by contrast stretching.

An examination of the corresponding images from Channel 4 clearly shows the ground but displays no evidence of these waves. PEELS lidar data from this time period as seen in Figure 8 shows no evidence of clouds or hazes in this region that could affect the background radiance. This same wave-like structure is also visible in the Channel 1 back-looking image but with a consistent time delay indicating that it is real and not some sort of unrecognized instrumental effect. Using Equation 1 and the observed time delay between forward- and back-looking scans, we estimate that the apparent altitude of the waves shown in Figure 8 are about 9 kilometers above sea level or 7 to 8 kilometers above the underlying mountainous topography.

We now believe that these 10-kilometer-scale waves are orographic in origin. Air moving over the mountainous terrain in Colorado and Utah is producing gravity waves that are propagating up into the troposphere where we observed them. This interpretation is bolstered by previous observations made by other investigators using totally different techniques who observed gravity waves under similar circumstances near mountains. These gravity waves had wavelengths on the order of 10 kilometers [6] – the same scale as the waves we have observed here. Whether the observed changes in radiance seen in Channel 1 are the result of temperature variations, differences in atmospheric water vapor content or a combination of these effects is still being investigated.

More interesting still are much smaller scale waves (<1 kilometer) such as those shown in Figure 16. This image has been calibrated, filtered and geometrically transformed to yield an undistorted view of this phenomenon. Faint arcs visible in the image are residual instrument noise that has been distorted by the geometric transformation process and made visible by stretching the contrast of the image. This 15 kilometer long image strip represents about 80 seconds worth of forward-looking data taken on Flight 9827 at about 00:32:30 UT on October 1, 1998.

The waves run diagonally through the image in Figure 16 and have maximum peak-to-trough amplitudes of only about 1.5% of the absolute scene radiance. These waves exhibit much lower contrast than the larger gravity waves just discussed making them much more difficult to spot. Unlike the larger waves, these waves have a more regular spacing with wavelengths on the order of only 400 meters.

As before, there is no evidence of these waves in the corresponding Channel 4 images and PEELS lidar data from this time, shown in Figure 6, show only a low lying marine cloud layer with an altitude of about 1 to 1.5 kilometers. There is no evidence in the lidar data for any other clouds that might be producing the observed variations in scene radiance. These same waves are also observed in the Channel 1 back-looking images again indicating that they are real. Based on the observed time delay between the forward- and back-looking Channel 1 images, these waves have an apparent altitude of 7.2 kilometers.

These and similar waves were seen during Flight 9827 from about 00:32 to 00:45 UT on October 1, 1998 over the Pacific Ocean off the coast of central California. The location of the ground track where these waves were observed is shown in Figure 17. This entire area is dominated by a low lying marine cloud layer at the time of our observations as can be seen in the PEELS lidar data presented in Figure 6.

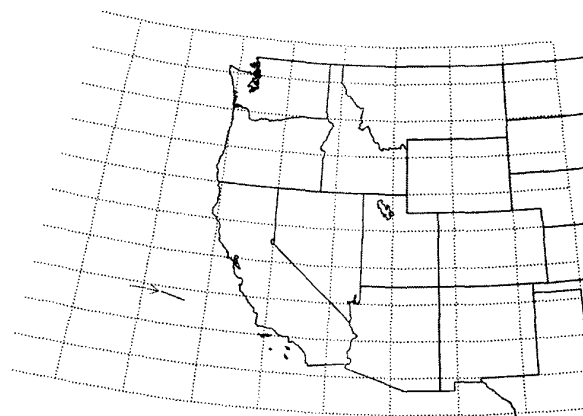


**Figure 17** Location of waves observed with subkilometer scales during flight 9827.

The origin of these waves is not as apparent as in the case of the gravity waves seen over the mountainous Southwest. There is no topography present and the presence of the relatively level marine cloud layer indicates that the atmosphere is quite stable especially at lower altitudes. The 400-meter wavelength is also much shorter than is typically associated with observed gravity waves.

One possible mechanism that is predicted to produce gravity waves with such short wavelengths and in this type of environment is some sort of wind shear in an otherwise stable atmosphere [6]. Our observations of these waves over the ocean with such short wavelengths appear to be unique. As with the ten-kilometer-scale waves observed over the Southwest, we are investigating if the observed changes in radiance observed in Channel 1 images are the result of temperature variations, differences in atmospheric water vapor content or a combination of these effects.

#### 4. CONCLUSIONS

The large amount of M/LWIR data gathered by the Aquameter during the FISTA 98 campaign presents a rich variety of atmospheric phenomenon that will allow us to verify and refine predictions of background clutter properties made by existing simulation programs under a range of conditions. The Aquameter's ability to simultaneously obtain forward- and back-looking images also gives us a unique capability to perform stereo imagery of these phenomena. Combined with supporting data from



other instruments (e.g. PEELS), this capability will allow us to ascertain the physical mechanisms responsible for what has been observed. Lessons learned from the FISTA 98 missions will be used to modify the Aquameter and supporting instruments as well as our experiment plans for the FISTA 99 mission currently scheduled for the end of 1999.

While the continuing characterization of the appearance of cloud edges as viewed in different spectral wavelengths has yielded some interesting insights, the discovery of clear air gravity waves observable only in the water band images was most unexpected. In addition, our stereo observations of less than kilometer-scale waves over the Pacific Ocean appears to be unique and should offer a glimpse at the origin of such waves. These data show that the Aquameter will be most useful in future investigations of wave-like structures in the troposphere.

## 5. ACKNOWLEDGEMENTS

The RAMOS research described herein is supported by BMDO under Contract No. HQ 0006-97-D-0002 to the Space Dynamics Laboratory, Utah State University (SDL/USU). Visidyne, Inc. supported SDL/USU under subcontract # C918574. The authors would like to thank the members of the Aquameter team at the Vavilov State Optical Institute, the FISTA flight team as well as Gary Jensen of SDL, Joe Kristl of SRL/SDL, Alexander Sidorin of Astroinform, and Pat McNicholl of Visidyne, Inc.

## 6. REFERENCES

- [1] A.J. LePage *et al.*, "IR/Visible Polarization Measurements of Scattered Solar Radiation from Clouds", *Proceedings of 1999 IEEE Aerospace Conference*, 1999
- [2] J. Lampe, "Capabilities of the Flying Infrared Signatures Technology Aircraft (FISTA)", *Proceedings of The Leonid MAC Workshop* (P. Jenniskens, ed.), 1999
- [3] V.S. Avduyevsky and G.R. Uspensky, *Scientific and Economy-Oriented Space Systems*, Mir Publishers (Moscow), 1988
- [4] See [www.visidyne.com/technologies/PEELS/peels.htm](http://www.visidyne.com/technologies/PEELS/peels.htm)
- [5] K. Sassen, "The Polarization LIDAR Technique for Cloud Research: A Review and Current Assessment", *Bulletin of the American Meteorological Society* 72, 1848, 1991
- [6] B.W. Atkinson, *Meso-Scale Atmospheric Circulations*, Academic Press, 1981

## 7. BIOGRAPHY



The lead author, Andrew J. LePage, is a Senior Scientist at Visidyne, Inc. specializing in computer image processing and analysis of remote sensing data. Since 1992, he has been involved in the development and implementation of image and optical data processing, analysis, and data visualization algorithms in support of a number of programs including RAMOS, MSX, CIRIS, IBSS, and EXCEDE III. Between 1987 and 1992 Mr. LePage was a Senior Engineer at Digital Equipment Corp. where he did innovative work on non-contact electrical testing using optical and high-powered laser technologies. While with Visidyne from 1985 to 1987, he was active in the design and fabrication of X-ray and IR optical systems for high altitude and space applications as well as development of image processing techniques to support research in variable MTF optical systems. Mr. LePage received his BS in Physics from the University of Lowell in 1985.